Bilge International Journal of Science and Technology Research
ISSN: 2651-401X
e-ISSN: 2651-4028
Research Article
2022, Volume: 6, Issue: 1, 16-19
Received: 13.07.2021; Accepted: 09.12.2021
DOI: 10.30516/bilgesci.971220

Investigation of Microstructural and Intrinsic Defect States of Facile Synthesized WO_3 Film

Orhan Emre Gülen[1], Emin Yakar[1], Fatma Sarf[2*]

Abstract: In this study, WO_3 films were simply deposited onto In:SnO_2 (ITO) substrates by chemical bath in acidic medium. Structural, mophological and optical properties of the synthesized WO_3 film were investigated by using x-ray diffraction (XRD), scanning electron microscope (SEM), atomic force microscope (AFM), photoluminescence (PL), Uv-Vis and Raman spectrophotometer. From x-ray patterns, the tungsten oxide coating exhibits a monoclinic phase structure. Relative homogeneous particle distribution of nanorod/nano-tooth mixed forms have been observed on the surface and also surface roughness is less compared to similar studies in the literature. Surface defect emission peaks esepecially oxygen vacancies are determined from PL spectrum. Green emission is attributed to heterogeneous film growth process. Raman spectra of the films is proof WO_3 formation. From these results, the aggregation–deposition mechanism is responsible to WO_3 film growth process.

Keywords: WO_3 film, chemical bath, structural, optical

[1]**Address:** Çanakkale Onsekiz Mart University, Engineering Faculty, Materials Science and Engineering, Çanakkale, Turkey
[2]**Address:** Çanakkale Onsekiz Mart University, Çan Vocational School, Çanakkale, Turkey

***Corresponding author**: fatmaozutok@comu.edu.tr

Citation: Gülen, O.E., Yakar, E., Sarf, F. (2022). Investigation of Microstructural and Intrınsıc Defect States of Facile Synthesized WO_3 Film. Bilge International Journal of Science and Technology Research, 6(1): 16-19.

1. INTRODUCTION

Metal oxide nanomaterials are known to exhibit improved optical, electrical and chemical reactivity properties compared to bulk counterparts (Pavia-Santos vd., 2021). Amog them, as an anode or cathode material (tungsten trioxide) WO_3 film is so preferable layer in electrochromic device applications due to its high coloration efficiency, transparent in oxidation state, deep blue in the reduction state and has a large number of coloration (Pooyodying vd., 2021). It exhibits a colour change according to this reaction;

$$WO_3 + xLi^+ + xe^- \rightarrow Li_xWO_3 \quad (1)$$

where WO_3 and Li_xWO_3 are transparent and absorbing, respectively. However WO_3 can not meet the color neutrality required for many smart window applications due to its blue color in the spectrum (Lagier vd., 2021). Therefore, controlled growth is targeted so that the optical properties of WO_3 films are improved to achieve high performance from them. At the same time, fast and efficient production is targeted

There are a lot of study including WO_3 films and their optical properties with using different techniques such as sol-gel, electrospinning and magnetron sputtering etc. (Hariharan vd., 2019). Recently, chemical bath deposition is very interesting among chemical film production methods because it is simple, allows large area application, inexpensive and does not need vacuum pump.

In this work, our goal is to investigate the growth process as well as to determine the intrinsic defect states of WO_3 films with using cost-effective chemical bath.

2. MATERIAL AND METHOD

ITO substrates were cleaned by detergent, alcohol and n-hexzane in ultrasonic bath along one hour. All chemicals were purchased from Sigma-Aldrich without further purification. Sodium tungsten dihydrate ($Na_2WO_4.2H_2O$)(≥% 99) was used as a tungsten source and HCl was used as a complex agent to adjust pH of the solution. In 100 ml. distilled water, 0.1 M W-source was dissolved and mixed on the magnetic stirrer. ITO substrates were immersed in aqueous solution and WO_3 films were grown into acidic bath solution (pH=2). Along the film synthesis process, working temperature and immersion time were 70±5 °C and 15 min. Finally, WO_3 film annealed at 500 ˚C for 2 h in the furnace. The crystal structure and measured structural parameters of the sample were determined by X-ray powder diffraction (XRD; Rigaku Smart Lab x-ray diffractometer; CuK_{α} radiation; 45 kV; 40 mA; step size 0.013˚) with powder method. Nanostructural investigation was done using scanning electron microscopy (SEM; JEOL JSM- 7100F; Au-Pd (80-20 %) coating) and atomic force microscopy (AFM;Witec Alpha 300 RA; non-contact mode). Surface elemental composition was determined by using energy-dispersive x-ray spectrometer (EDX; OXFORD Instruments X-Max) which was attached to SEM. UV-Vis spectra of the samples was investigated between 300-900 nm range. Optical parameters (T and A) was investigated by Analytic Jena Uv-Vis spectroscopy in the 300-900 nm. range. Photoluminescence emission measurements were realized by ANDOR SR500i-BL with excitation wavelength of 349 nm. Raman spectrophotometer (Thermo DXR) was used to confirm the degree of microstructural disorder.

3. RESULTS

Figure 1 shows the x-ray patterns of the produced film. The sharp peaks indicate that the as-synthesized products are well-crystallized. ITO-based peak and W-related peak are observed in the 2θ= 65˚-70˚ and 2θ= 45˚-50˚ range, respectively due to less crystal nuclei at pH value of 2.0 (Lu vd., 2014). According to JCPDS Card No: 43-1035, characteristic three monoclinic WO_3 phase peaks of (001), (020) and (200) are detected between 2θ= 25˚-30˚ and (220) peak is observed in the 2θ= 30˚-35˚ range. From these results, retention level of WO_3 film onto ITO substrate is high.

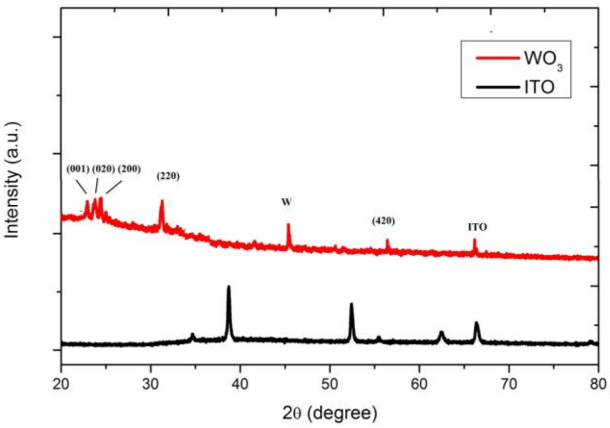

Figure 1. X-ray patterns of WO_3 film in the 2θ= 20˚-80˚ range

In Figure 2., surface image of the WO_3 film is shown. Relatively homogeneous and smooth surface is observed with mixed nanorod/nano-tooth forms due to some particles are growing fast, but others are growing slowly. Nanorod forms are associated with the crystal planes are parallel to the c axis WO_3 crystal nucleus. Observed nano-tooth forms can provide porosity on the surface, thus increasing the surface/volume ratio. It may be useful due to functionality of material is strongly depends on surface morphology.

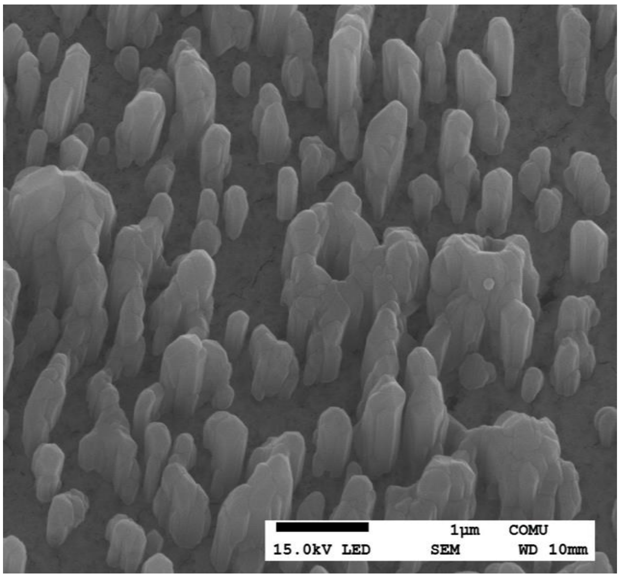

Figure 2. Surface morphology of WO_3 films

Elemental analysis results are given as below in Figure 3. It is proof that tungsten and oxygen peaks are recorded. Sodium and sulphur peaks are shown due to low solubility of W-source aqueous solution whereas annealing process is applied to remove surface impurities.

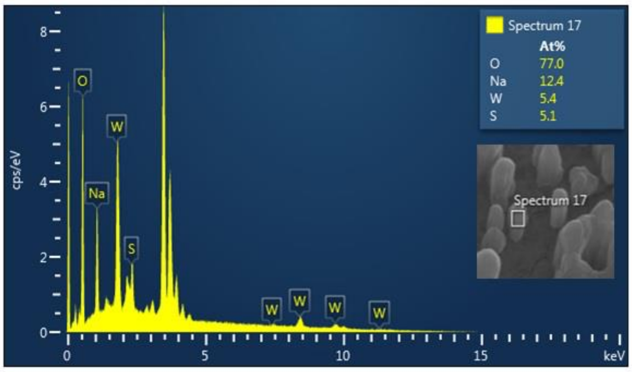

Figure 3. Elemental analysis results WO_3 films

Figure 4 shows that two dimension (2D) and three dimension (3D) AFM images of WO_3 film. It is kown that surface roughness is so important for optical studies (Ramkumar vd., 2016). Surface roughness values of SA and SQ are 16.02 nm and 19.29 nm, respectively. From this result, surface roughness of the synthesized sample is lower than compared to literatüre (Babu, 2016). When looking at both 2D and 3D AFM images, the particle distribution is relatively uniform and agglomeration of atoms on the surface can cause the formation of large grains which correlated to SEM images.

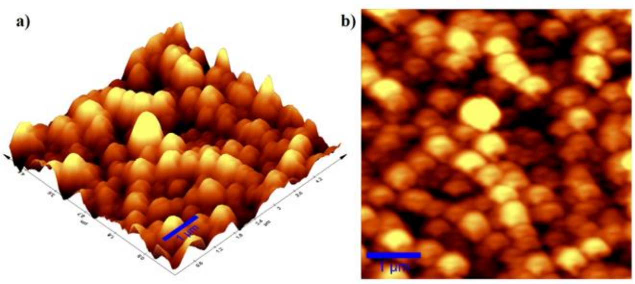

Figure 4. 3D (a) and 2D (b) surface topography of WO_3 films

Figure 5 exhibit the PL emission spectra of WO_3 film which measuring between 350 to 800 nm with 349 nm excitation wavelength of Nd–YLFQ laser. A series of peak are detected at 432, 522, 574 and 700 nm which may be attributed to surface defect related peaks. Emission peaks of surface defects are often associated with oxygen vacancies and tungsten interstitial sites, as generalized in metal oxides.

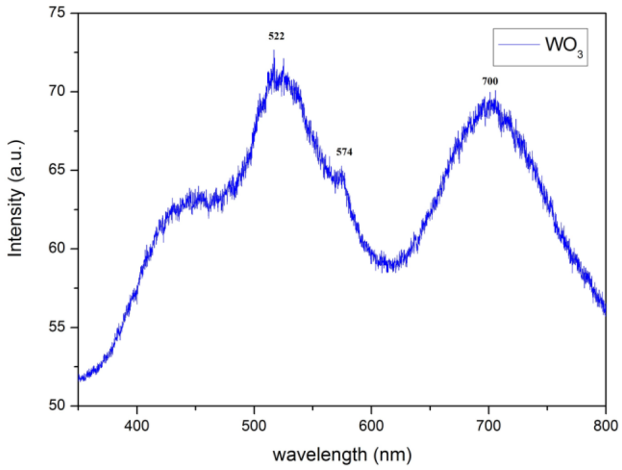

Figure 5. PL spectrum of WO_3 films

In Figure 6, Raman spectra of WO_3 films, which is sited at range 200-1200 cm^{-1}. Symmetric streching mode of W=O is observed in the 950-1050 cm^{-1} range (Díaz-Reyes, 2008). Crystalline WO_3 phase is determined in 806 cm^{-1} which corresponds to stretching vibrations of the bridging oxygen (Tagtstrom, 1999). δ(O–W–O) bending modes are determined in the 200-400 nm range (Ou, 2011). Impurity based peaks are determined in in the 400-700 cm^{-1} range.

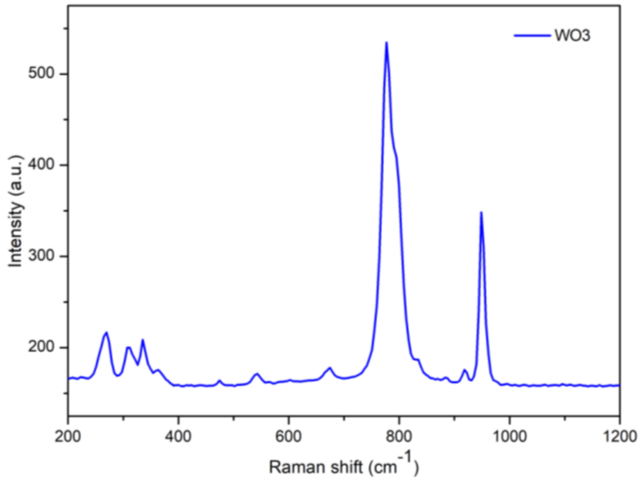

Figure 6. Raman spectrum of WO_3 films

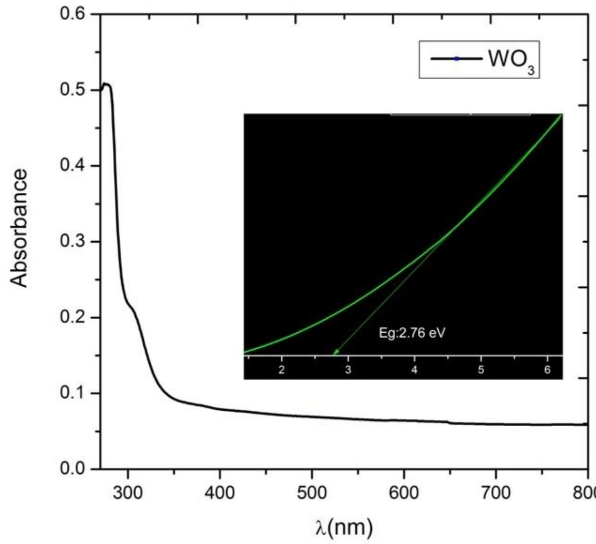

Figure 7. Uv-Vis spectrum and optical band of WO_3 film

In Figure 7, Uv-Vis spectra in the 300-900 nm range and opitcal band gap of WO_3 film is shown. The wide optical absorption band in the optical transmittance spectra of the deposited WO_3 film is attributed to the presence of tungsten ions with the W^{5+} states (Zou, 2014). Low optical band gap value of 2.7 eV is proper for opto-electronic device applications.

4. DISCUSSION AND CONCLUSIONS

Herein, WO_3 film was deposited by chemical bath deposition and structural, morphological and optical properties of the WO_3 film were investigated in detail. Monoclinic WO_3 crystal phase from XRD, W and O indexed peaks from elemental analysis and optical phonon modes of W-O from Raman spectrum are evidence of the WO_3 film production. Nanorod and nano-tooth forms are exhibited whn investigated surface images. Oxygen vacancy correlated defect energy states are determined at 522, 574 and 700 700 nm. According to the obtained results, the aggregation–deposition mechanism can be explain the WO_3 film growth process under film deposition parameters (complex agent was HCl, W-source was sodium tungsten dihydrate, pH=2, T=70 °C, t=15 min.)

Ethics Committee Approval
N/A

Peer-review
Externally peer-reviewed.

Author Contributions
All authors have read and agreed to the published version of manuscript.

Conflict of Interest
The authors have no conflicts of interest to declare.

Funding
The authors declared that this study has received no financial support.

REFERENCES

Babu, M.B., Madhuri, K.V. (2016). Structural, morphological and optical properties of electron beam evaporated WO_3 thin films. Journal of Taibah University for Science, 1232-1237.

Escalante, G., López, R., Noé F., Demesa, Gerardo Villa-Sánchez, Víctor Hugo Castrejón-Sánchez, Vivaldo de la Cruz, I. (2021). Correlation between Raman spectra and color of tungsten trioxide (WO_3) thermally evaporated from a tungsten filament, AIP Advances, 11, 055103.

Díaz-Reyes, J.,, Dorantes-García, V., Pérez-Benítez, A., Balderas-López, J.A.(2008). Obtaining of films of tungsten trioxide (WO3) by resistive heating of a tungsten filament Superficies y Vacío, 21(2) 12-17.

Hariharan, V., Gnanavel, B., Sathiyapriya, R., Aroulmoji, V. (2019). A Review on Tungsten Oxide (WO_3) and their Derivatives for Sensor Applications. International journal of advanced Science and Engineering, 5, 1163-1168.

Lagier, M., Bertionotti, A., Bouvard, O., Burnier, L., Schaler, A. (2021). Optical properties of in vacuo lithiated nanoporous WO_3:Mo thin films as determined by spectroscopic ellipsometry. Optical Materials, 117,11091.

Lu, C., Hon, M.H., Kuan, C., Leu, I. (2014). Preparation of WO_3 nanorods by a hydrothermal method for electrochromic device. Japanese Journal of Applied Physics, 53, 06JG08, 1-5.

Ou, Z., Yacoob, M.H., Breedon, M., Zheng, H.D., Campell, J.L., Latham, K., Plessis, J., Wlofarski, W., Kalantar-Kadeh, K. (2011). *In situ*Raman spectroscopy of H_2 interaction with WO_3 films. Phys. Chem. Chem. Phys., 13, 7330-7339.

Ramkumar, S., Rajarajan, G. (2016). Effect of Fe doping on structural, optical and photocatalytic activity of WO_3 nanostructured thin films. J Mater Sci: Mater Electron, 27, 1847–1853.

Zou, Y.S., Zhang, Y.C., Lou, D., Wang, H.P., Gu, L., Dong, Y.H., Dou, K., Song, X.F., Zeng H.B. (2014). Structural and optical properties of WO3 films deposited by pulsed laser deposition. Journal of Alloys and Compounds, 583, 465-470.